Advanced Journal of Chemistry, Section A

Journal homepage: www.ajchem-a.com

Original Article

Computational Multi-Target Profiling of Lupeol against Cardiometabolic Diseases: An Integrated Docking, Network Pharmacology, and Molecular Dynamics Approach

Pavithra Velusamy[1,2]*, S. Rani[1], G. Ariharasivakumar[2]

[1]*Department of Pharmacy, Annamalai University, Chidambaram, Tamil Nadu, India*
[2]*Department of Pharmacology, KMCH College of Pharmacy, Coimbatore, Tamil Nadu, India*

ARTICLEINFO

Article history

Submitted: 2025-11-27
Revised: 2026-01-08
Accepted: 2026-01-25
ID: AJCA-2511-1984
DOI: 10.48309/AJCA.2026.545279.1984

KEYWORDS

Lupeol
Cardiometabolic diseases
Network pharmacology
Molecular docking
Molecular dynamics
PI3K–Akt signalling

ABSTRACT

Cardiometabolic diseases (CMDs), including type 2 diabetes, obesity, and cardiovascular disorders, share interlinked pathogenic mechanisms involving chronic inflammation, insulin resistance, oxidative stress, and endothelial dysfunction. Multi-target agents derived from natural compounds offer promising therapeutic avenues for CMD management. Lupeol, a pentacyclic triterpenoid, has demonstrated diverse bioactivities; yet, its mechanistic relevance in CMDs has not been comprehensively elucidated. This study aimed to elucidate the multitarget pharmacological potential of lupeol against CMDs through an integrated computational approach encompassing network pharmacology, computational docking, and dynamic simulation. Lupeol- and CMD-associated targets were retrieved from various databases and analyzed via protein–protein interaction (PPI) analysis using Cytoscape. Functional enrichment was performed using DAVID and Metascape. Drug-likeness and toxicity were assessed through SwissADME and ADMETlab 2.0. Binding affinities were evaluated using computational docking, followed by MD simulations and specific tissue expressions to validate complex stability. A total of 179 shared targets were identified, with STAT3, MAPK3, ESR1, EGFR, and CXCR4 emerging as key hub genes. GO and KEGG enrichment highlighted significant involvement in PI3K–Akt, MAPK, JAK–STAT, and AGE–RAGE regulatory pathways. Lupeol exhibited strong interaction energies (–9.08 to –6.08 kcal/mol) and stable interactions with major CMD targets. ADME-Tox profiling demonstrated its oral bioavailability, BBB permeability, and low toxicity risk. MD simulations showed stable protein–ligand conformations under near-physiological conditions. Collectively, these findings highlight lupeol as a promising multi-target lead compound for CMD management and provide a robust computational foundation for its future experimental and translational evaluation.

* Corresponding author: Velusamy, Pavithra
✉ E-mail: pavithravelusamy711@gmail.com

GRAPHICAL ABSTRACT

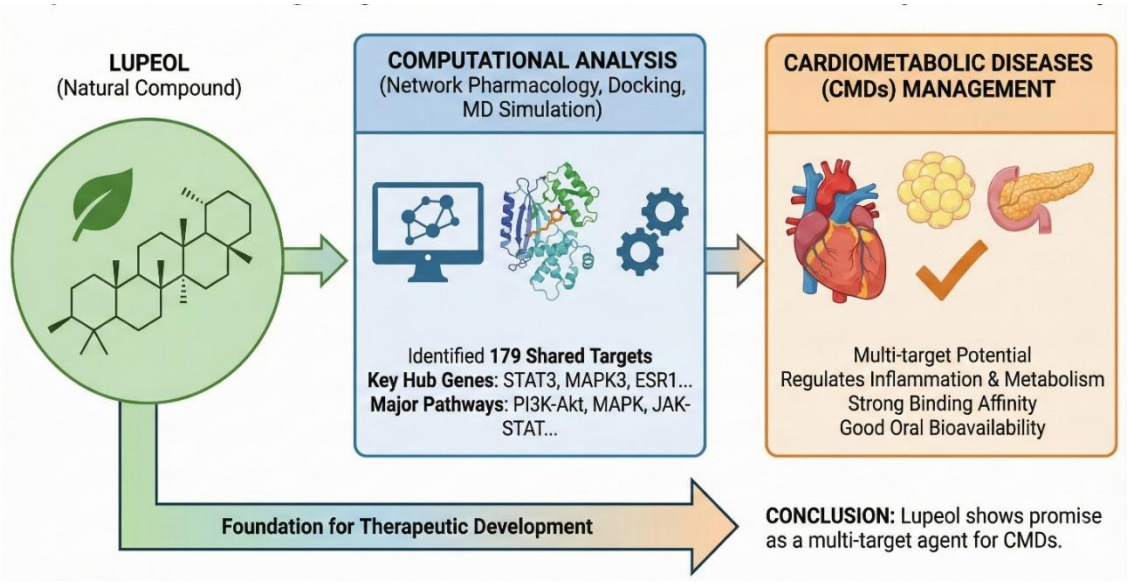

Introduction

Cardiometabolic diseases (CMDs), including type 2 diabetes mellitus (T2DM), coronary artery disease (CAD), hypertension, obesity, and dyslipidemia, represent a major public health burden globally. The CMDs prevalence has been increasing steadily, driven by sedentary lifestyles, unhealthy diets, and aging populations. Collectively, these conditions account for the majority of non-communicable disease-related morbidity and mortality worldwide [1]. Notably, the coexistence of two or more of these conditions—referred to as *cardiometabolic multimorbidity (CMM)*—has been associated with a markedly increased risk of myocardial infarction, stroke, renal failure, and premature death [2,3].

Despite advances in therapeutics, current treatment approaches remain largely focused on single-target interventions. Commonly prescribed agents such as statins, beta-blockers, angiotensin-converting enzyme (ACE) inhibitors, and metformin have demonstrated clinical benefits; yet, they often fail to address the multifactorial and interconnected molecular mechanisms underlying CMD pathogenesis [4,5]. These drugs also present concerns regarding long-term efficacy, side effects, and polypharmacy. These limitations have driven growing interest in multi-target therapeutic strategies capable of modulating complex disease networks rather than isolated molecular targets. Phytochemicals derived from dietary and medicinal plants have gained considerable attention as potential multi-target agents for chronic metabolic disorders. Among these, lupeol, a pentacyclic triterpenoid abundantly present in mango (*Mangifera indica*), olive (*Olea europaea*), *Crataeva nurvala*, and *Betula* species, has been widely reported to exhibit diverse pharmacological activities [6–8]. Experimental studies have demonstrated lupeol's antioxidant, anti-inflammatory, antidiabetic, anti-atherosclerotic, hepatoprotective, and cardioprotective properties [9,10]. These biological effects have been suggested to involve modulation of multiple signaling cascades, including NF-κB, PI3K–Akt, MAPK, JAK–STAT, and insulin signaling pathways, all of which are critically implicated in CMD progression [11].

However, despite these promising findings, the precise molecular mechanisms underlying lupeol's protective role in CMDs have not yet been

comprehensively elucidated. Most available studies have focused on isolated biological endpoints, thereby failing to capture the broader, system-level interactions through which lupeol may exert its therapeutic effects. In this context, network pharmacology has emerged as a powerful computational strategy that enables the systematic exploration of compound–target–pathway interactions within complex disease networks [12]. When integrated with molecular docking and molecular dynamics (MD) simulations, this approach provides valuable insights into ligand–protein binding behavior, structural stability, and potential functional relevance at the molecular level [13].

Based on these considerations, we hypothesized that lupeol may interact with multiple pathogenic targets involved in CMDs and modulate key regulatory pathways associated with inflammation, oxidative stress, and metabolic dysregulation. To test this hypothesis, the present study employed an integrated computational framework combining network pharmacology analysis, functional enrichment profiling, molecular docking, and 100-ns MD simulations. This multi-tiered strategy was designed to systematically characterize the multi-target potential of lupeol against CMD-associated molecular networks and to provide a mechanistic foundation for future experimental validation.

Materials and Methods

Identification of CMD-associated targets

Genes associated with CMDs, including T2DM, CAD, atherosclerosis, hypertension, and dyslipidemia, were retrieved from publicly available databases, namely DisGeNET and GeneCards. Relevant keywords such as *"cardiometabolic disease," "type 2 diabetes," "coronary artery disease," "hypertension,"* and *"dyslipidemia"* were used for database querying. From the GeneCards database, genes with relevance scores greater than 10 were selected to ensure biological significance. All retrieved gene symbols were normalized using the UniProt database to maintain consistency and accuracy in downstream analyses [14].

Identification of lupeol-associated targets

Potential protein targets of lupeol were predicted using SwissTargetPrediction, BindingDB, and the comparative toxicogenomics database (CTD). The canonical SMILES structure of lupeol (PubChem CID: 259846) was obtained from the PubChem database and used as the input structure for target prediction. Duplicate and redundant targets were removed, and all remaining protein targets were standardized using UniProt identifiers to ensure uniform annotation across databases [15].

Target intersection and venn analysis

To identify the potential therapeutic targets of lupeol in CMDs, the intersection between lupeol-associated targets and CMD-related genes was determined. A Venn diagram was generated using Venny 2.1.0 to visualize overlapping gene sets. The intersecting genes were considered putative targets through which lupeol may exert its cardiometabolic regulatory effects.

Construction and analysis of protein–protein interaction network

The overlapping gene targets were uploaded to the STRING database to construct a protein–protein interaction (PPI) network, with the confidence score threshold set at >0.7. The resulting PPI network was imported into Cytoscape v3.10.3 for visualization and network analysis. Topological parameters, including degree centrality, betweenness centrality, and clustering coefficient, were calculated using the CytoHubba plugin. Core hub targets were identified based on higher degree values,

reflecting their potential regulatory importance within the CMD network [16]

Drug-likeness and toxicity prediction

The pharmacokinetic properties and drug-likeness of lupeol were evaluated using SwissADME and ADMETlab 2.0 web servers. The canonical SMILES of lupeol was used as input. Drug-likeness was assessed according to Lipinski's Rule of Five, considering molecular weight, hydrogen bond donors and acceptors, topological polar surface area (TPSA), and octanol–water partition coefficient (log P) [17]. Toxicological parameters, including hERG channel inhibition, human hepatotoxicity, respiratory toxicity, eye corrosion, and rat oral acute toxicity, were predicted using ADMETlab 2.0. All ADME–toxicity parameters were systematically recorded and interpreted to evaluate lupeol's suitability as a drug-like candidate [18].

Gene ontology and KEGG pathway enrichment analysis

Functional enrichment analysis was performed on the overlapping lupeol–CMD targets using the DAVID 6.8 database. Gene ontology (GO) terms were categorized into biological processes (BP), cellular components (CC), and molecular functions (MF). Kyoto encyclopedia of genes and genomes (KEGG) pathway enrichment was conducted, and pathways with $p < 0.05$ were considered statistically significant. Enrichment visualization was performed using Bioinformatics, and the most relevant pathways were selected for further network interpretation [19].

MCODE clustering analysis

To identify densely connected gene modules within the PPI network, MCODE (Molecular Complex Detection) clustering analysis was performed using Metascape. Cluster selection was based on MCODE scores, enrichment p-values (< 0.05), and degree cutoffs. The resulting clusters were analyzed to identify functionally relevant gene modules associated with cardiometabolic regulation [20].

Construction of the Compound–Target–Pathway Network

A compound–target–pathway interaction network was constructed using Cytoscape v3.10.3, integrating lupeol, top-enriched KEGG pathways, and their associated target genes. Network topological parameters were evaluated to identify hub nodes. Core targets were finalized by intersecting high-ranking nodes from both the PPI network and the compound–pathway network.

Molecular docking

Molecular docking simulations were performed using Schrödinger Glide (SP mode) to evaluate binding interactions between lupeol and selected CMD-associated target proteins. Three-dimensional crystal structures of target proteins were retrieved from the RCSB Protein Data Bank. Protein preparation was conducted using the Protein Preparation Wizard, including removal of water molecules, addition of hydrogen atoms, and energy minimization. Docking grids were generated around the active binding sites, and docking scores were expressed in kcal/mol to rank binding affinities [22-24].

MD *simulation*

MD simulations were carried out using the Desmond v5.6 module of Schrödinger to assess the stability of lupeol–protein complexes. Each complex was solvated in an orthorhombic box using the TIP3P water model, and counter-ions were added to neutralize the system under physiological salt concentration (0.15 M NaCl).

The OPLS3e force field was applied, and simulations were performed for 100 ns under NPT ensemble conditions (300 K, 1 atm). Trajectory analyses were conducted for root mean square deviation (RMSD), root mean square fluctuation (RMSF), radius of gyration (Rg), solvent-accessible surface area (SASA), hydrogen bonding, and secondary structure stability [21].

Tissue-specific expression analysis

To assess biological relevance, tissue-specific expression levels of hub genes (CXCR4, EGFR, FGF2, ESR1, and MAPK3) were retrieved from the Human Protein Atlas database. Expression values were recorded as normalized transcripts per million (nTPM) for CMD-relevant tissues, including heart, liver, adipose tissue, and pancreas. Bar plots were generated to visualize relative expression distributions across tissues.

Results

Identification of CMD-associated targets

A total of 10,440 CMD-associated genes were retrieved from the DisGeNET and GeneCards databases using disease-related keywords such as *"type 2 diabetes mellitus," "coronary artery disease," "hypertension," "dyslipidemia," "atherosclerosis,"* and *"heart failure."* After normalization using the UniProt database and removal of duplicate entries, the final gene set was considered representative of the molecular landscape associated with CMD pathophysiology.

Identification of lupeol targets and intersection with CMD genes

A total of 1,797 protein targets associated with lupeol were identified from Swiss Target Prediction, Binding DB, and the Comparative Toxicogenomic Database using its canonical SMILES structure. Intersection analysis between lupeol-associated targets and CMD-related genes revealed 179 common targets, which were visualized using a Venn diagram (Figure 1).

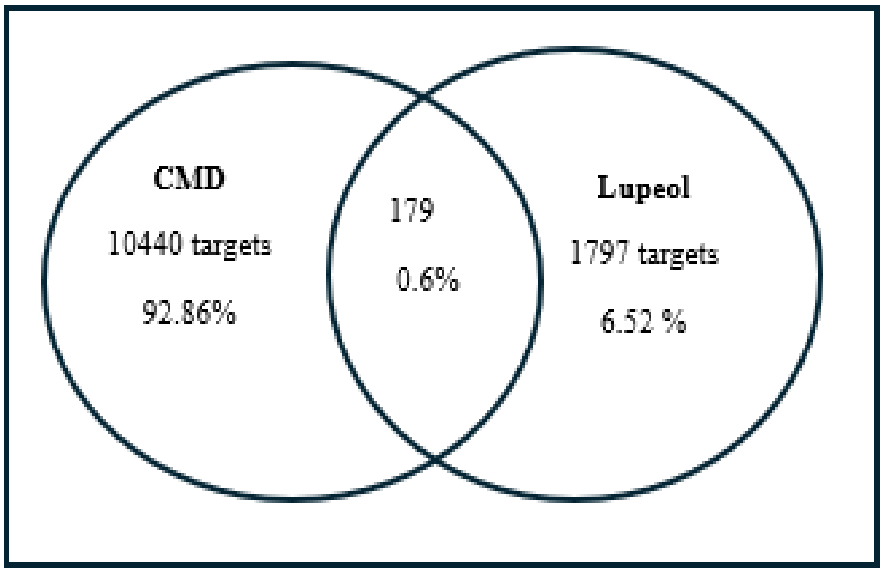

Figure 1. Venn diagram illustrating the overlap between lupeol-associated targets and CMDs–related genes. A total of 179 common targets were identified by intersecting 1,797 lupeol-predicted proteins with 10,440 CMD-associated genes, highlighting the potential multi-target pharmacological relevance of lupeol

These overlapping genes were considered putative therapeutic targets through which lupeol may exert multi-target regulatory effects in CMDs.

PPI network analysis

To investigate the interaction landscape among the overlapping targets, the 179 common genes were imported into the STRING database with a confidence score threshold set at >0.7. The resulting PPI network consisted of 167 nodes and 1,235 edges and was visualized using Cytoscape v3.10.3. Topological analysis using the CytoHubba plugin identified the top 20 hub genes based on degree centrality, including STAT3, GSK3B, ESR1, JAK2, NFKB1, and SIRT1. These hub proteins are known to participate in inflammatory signaling, oxidative stress regulation, insulin signaling, and metabolic homeostasis, all of which are critically involved in CMD progression. To further illustrate these relationships, a compound–target interaction network was constructed (Figure 2), followed by visualization of hub gene distribution (Figures 3 and 4).

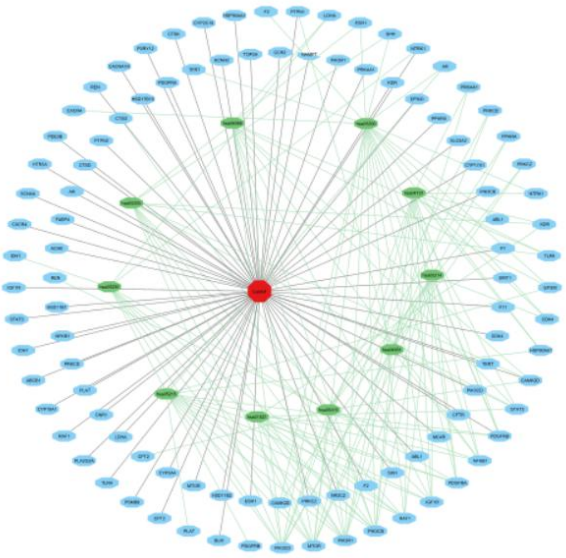

Figure 2. Compound–target interaction network illustrating the associations between lupeol (central node) and prioritized CMD-related protein targets. The network was constructed using Cytoscape v3.10.3

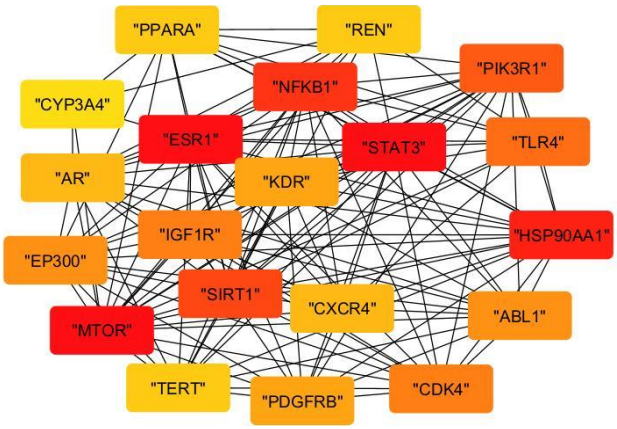

Figure 3. PPI network highlighting the top 20 hub genes identified by CytoHubba using the degree algorithm. Nodes are coloured according to degree values, with red indicating higher connectivity

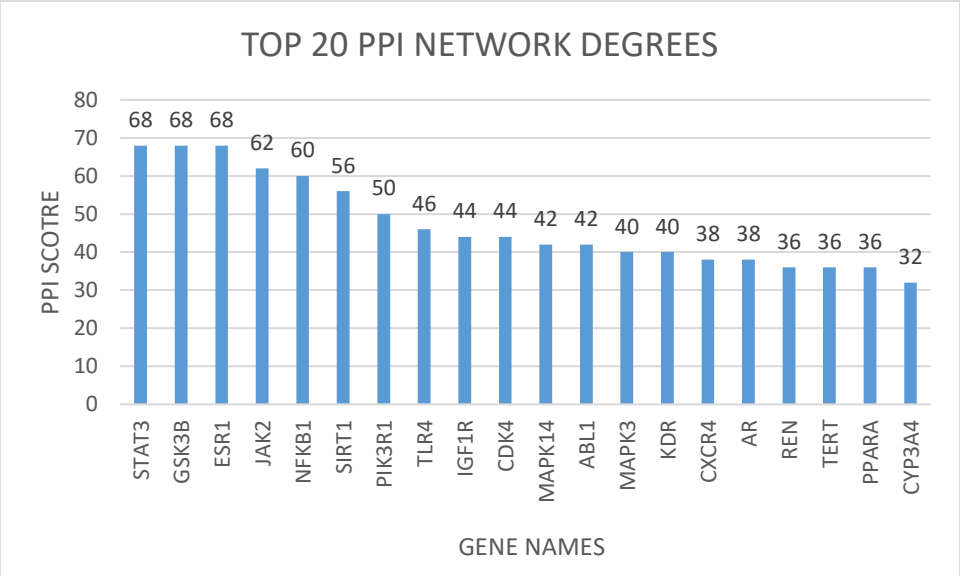

Figure 4. Bar graph representing degree centrality scores of the top 20 hub genes within the lupeol–CMD PPI network. STAT3, GSK3B, and ESR1 exhibited the highest degree values, indicating their potential central regulatory roles

Drug similarity and toxicity analysis

The pharmacokinetic and safety properties of lupeol were evaluated using SwissADME and ADMETlab 2.0 platforms. Lupeol demonstrated favourable oral absorption, acceptable drug-likeness, and a low predicted toxicity profile, supporting its suitability as a potential drug-like candidate. Table 1 shows *in silico* ADME and toxicity profile of lupeol. Radar plot summarizing key pharmacokinetic and toxicity parameters is illustrated in Figure 5.

Absorption and distribution

Lupeol exhibited high predicted human intestinal absorption (95.78%) and good Caco-2 permeability, although it showed low aqueous solubility (log S = –5.861), which is typical of lipophilic triterpenoids. Blood–brain barrier permeability was predicted, and plasma protein binding was estimated at 87.89%, indicating strong systemic distribution potential.

Metabolism and excretion

Lupeol was predicted to be a substrate of CYP3A4, suggesting hepatic metabolism, but did not inhibit major cytochrome P450 isoforms, including CYP1A2, CYP2C19, CYP2C9, and CYP2D6. Total clearance was predicted to be low (log 0.153), and lupeol was not identified as a renal OCT2 substrate, suggesting limited renal elimination.

Toxicity

Toxicity prediction analyses indicated that lupeol is non-mutagenic, non-hepatotoxic, and does not inhibit hERG I or II channels, suggesting a favourable cardiac safety profile. Acute (LD_{50} = 2.563 mol/kg) and chronic (LOAEL = 0.89 log mg/kg/day) toxicity values were within acceptable limits. Collectively, these results support the potential safety and tolerability of lupeol for systemic use.

Table 1. *In silico* drug-likeness and toxicity prediction of lupeol

Category	Parameter	Predicted value	Interpretation
Absorption	Water solubility	–5.861 log mol/L	Poor (typical for lipophilic compounds)
	Caco-2 permeability	1.226 log Papp	Good intestinal permeability
	Human intestinal absorption	95.78%	High oral absorption
	Skin permeability	–2.744 log Kp	Poor dermal permeability
	P-gp substrate	No	Not affected by efflux
	P-gp I/II inhibitor	Yes / Yes	May enhance uptake of co-administered drugs
Distribution	BBB penetration	Yes	Capable of CNS access
	Plasma protein binding	87.89%	High systemic binding
	Fraction unbound	1.69%	Moderate availability
	VDss (log L/kg)	1.64	Moderate distribution
Metabolism	CYP3A4 substrate	Yes	Metabolized hepatically
	CYP inhibition (1A2, 2C19, etc.)	No	No major inhibition (low DDI risk)
Excretion	Total clearance	0.153 log ml/min/kg	Low metabolic clearance
	OCT2 substrate	No	Not eliminated via renal OCT2
Toxicity	AMES toxicity	No	Non-mutagenic
	hERG I/II inhibition	No / No	Safe cardiac profile
	Oral rat acute toxicity (LD_{50})	2.563 mol/kg	Moderate acute safety
	LOAEL (Chronic)	0.89 log mg/kg/day	Low chronic toxicity
	Hepatotoxicity	No	Non-hepatotoxic
	Skin sensitisation	No	Dermatologically safe
	T. pyriformis toxicity	0.316 log µg/L	Moderate environmental toxicity
	Minnow toxicity	–1.696 log mM	Low aquatic toxicity

GO and KEGG pathway enrichment analysis

Gene enrichment analysis was performed on the 179 overlapping lupeol–CMD targets using the DAVID 6.8 database and Metascape platform to elucidate their biological functions and pathway associations.

GO enrichment

A total of 2,614 GO terms were significantly enriched, comprising 972 biological process (BP), 92 molecular function (MF), and 59 cellular component (CC) terms ($p < 0.05$) (Figure 6A).

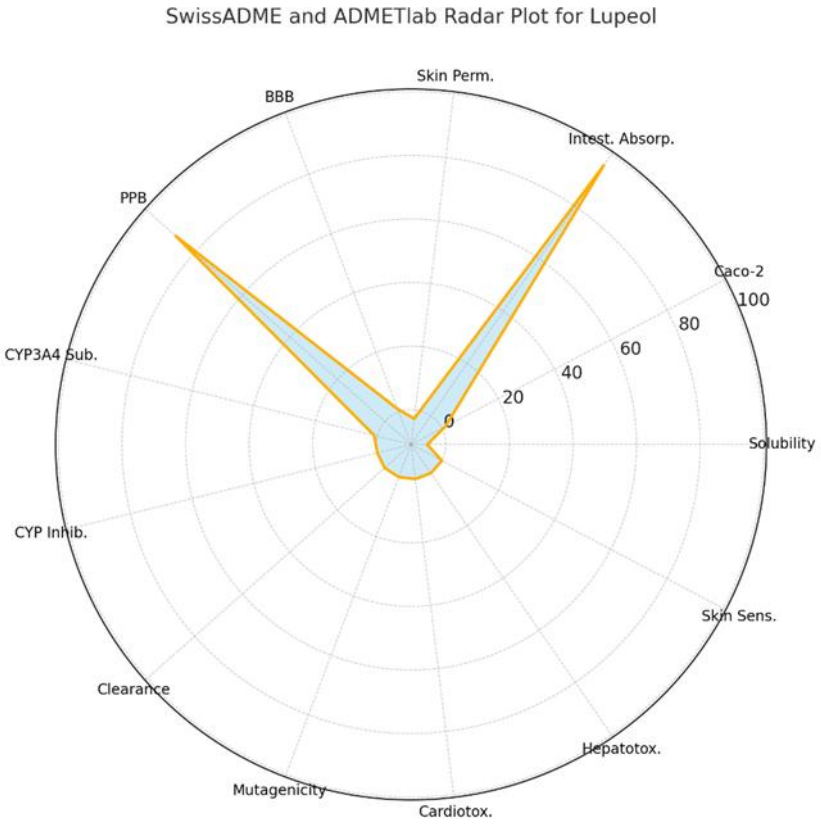

Figure 5. Radar plot summarizing key pharmacokinetic and toxicity parameters of lupeol, demonstrating high intestinal absorption, favourable permeability, and low predicted toxicity

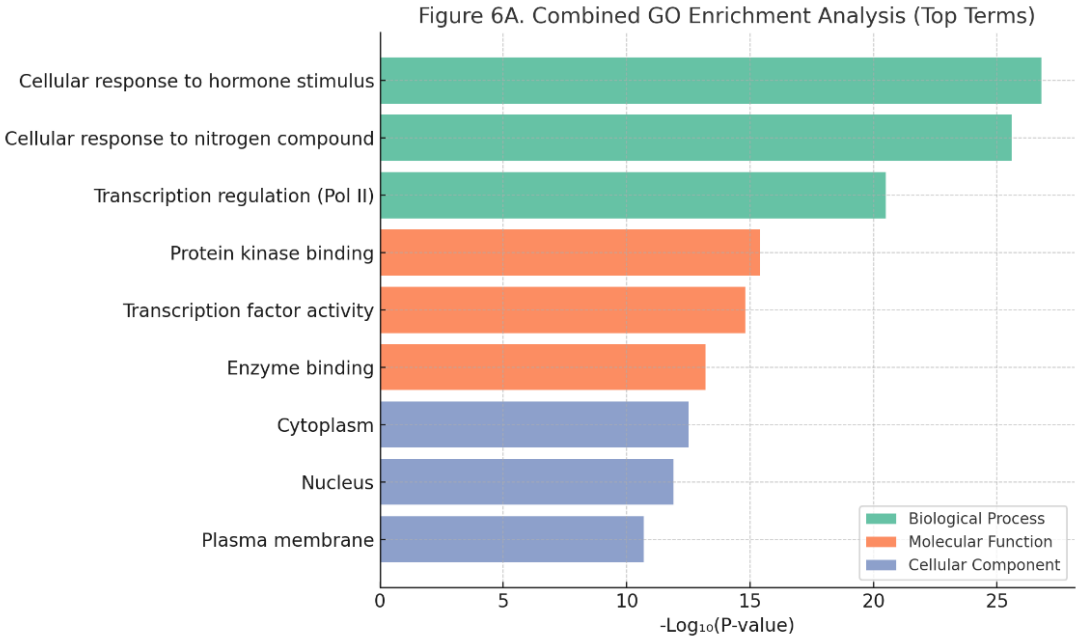

Figure 6A. Bar chart representing the top enriched GO terms across BP, MF, and CC. Statistical significance is expressed as $-\log_{10}$(p-value)

The enriched BP terms were primarily associated with cellular response to oxidative stress, regulation of inflammatory response, protein phosphorylation, insulin receptor signaling, and regulation of apoptosis, all of which are central to CMD pathophysiology. MF terms were mainly related to kinase activity, receptor binding, and transcription factor binding, while CC terms highlighted membrane rafts, cytosol, nucleus, and protein-containing complexes. These results indicate that lupeol-associated CMD targets are involved in diverse BP spanning metabolic regulation, inflammatory signaling, and cellular stress responses.

KEGG pathway enrichment

KEGG pathway enrichment analysis identified 146 significantly enriched pathways ($p < 0.05$) (Figure 6B). Among these, several pathways closely associated with CMD development and progression were prominently represented, including:

- PI3K–Akt regulatory pathway (hsa04151)
- MAPK regulatory pathway (hsa04010)
- AGE–RAGE regulatory pathway in diabetic complications (hsa04933)
- JAK–STAT regulatory pathway (hsa04630)
- HIF-1 regulatory pathway (hsa04066)
- TNF signaling, FoxO, insulin, and adipocytokine pathways

These pathways are critically involved in the regulation of glucose homeostasis, lipid metabolism, inflammation, endothelial function, and cellular survival, which are hallmarks of CMD pathogenesis.

To further contextualize the enrichment results, a schematic representation of the PI3K–Akt signaling pathway was generated to highlight the integration of lupeol-associated targets within this regulatory cascade (Figure 6C). Activation of PI3K leads to downstream Akt phosphorylation, which modulates glucose metabolism, protein synthesis, cell survival, and inflammatory responses, underscoring its relevance to CMD pathophysiology.

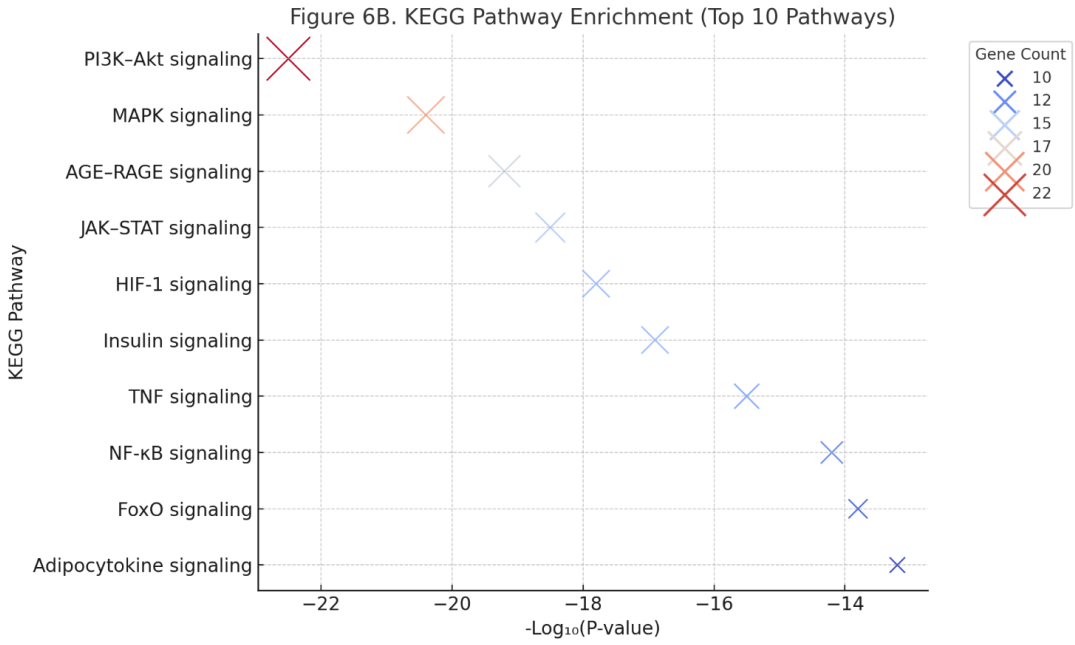

Figure 6B. Bubble plot illustrating the top 10 enriched KEGG pathways among lupeol–CMD targets. Bubble size represents the number of associated genes, while colour intensity reflects statistical significance ($-\log_{10}$ p-value)

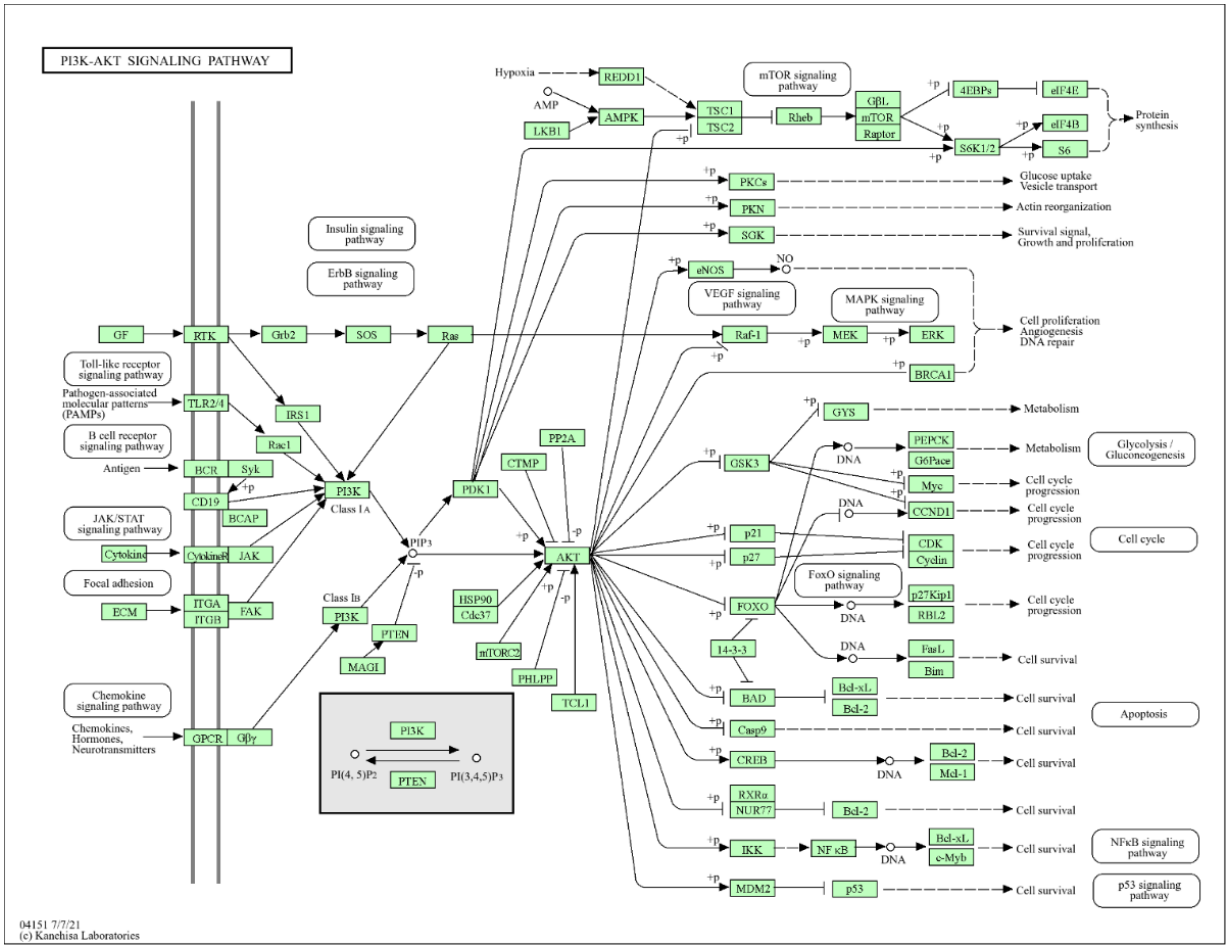

Figure 6C. Schematic overview of the PI3K–Akt signaling pathway highlighting key lupeol–CMD target genes involved in metabolic and inflammatory regulation

Metascape-based MCODE clustering

To identify densely connected functional modules within the PPI network, MCODE clustering analysis was conducted using the Metascape platform. Two major gene clusters with high MCODE scores and significant enrichment values were identified. MCODE Cluster 1 was enriched for pathways related to EGFR tyrosine kinase inhibitor resistance, cancer-associated signaling, and receptor-mediated phosphorylation events, suggesting strong involvement in cell proliferation and survival signaling. MCODE Cluster 2 showed enrichment in proteoglycans in cancer, HIF-1 signaling, and phosphorylation-related BP, indicating roles in angiogenesis, hypoxia response, and metabolic adaptation. These clusters highlight functionally cooperative subnetworks that may contribute to CMD progression through interconnected signaling pathways (Figure 6D).

Functional subnetwork and MCODE clustering analysis

To further explore system-level interactions, functional subnetworks were constructed using Metascape, integrating enriched BP and pathway associations. The resulting network (Figure 6E) highlighted key biological themes, including cellular response to nitrogen compounds, FOXO signaling, leptin signaling, regulation of metabolic processes, and apoptotic regulation. Furthermore, the integration of MCODE clustering

results revealed two principal regulatory modules (Figure 6F).

- Module 1 comprised STAT3, JAK2, FGFR1, and associated nodes, which are known regulators of inflammatory and cytokine-mediated signaling.
- Module 2 included EGFR, ESR1, MAPK3, and related proteins involved in growth factor signalling, metabolic regulation, and vascular function.

The identification of these tightly connected modules supports the hypothesis that lupeol may exert cardiometabolic regulatory effects through coordinated modulation of multiple signaling hubs rather than single isolated targets.

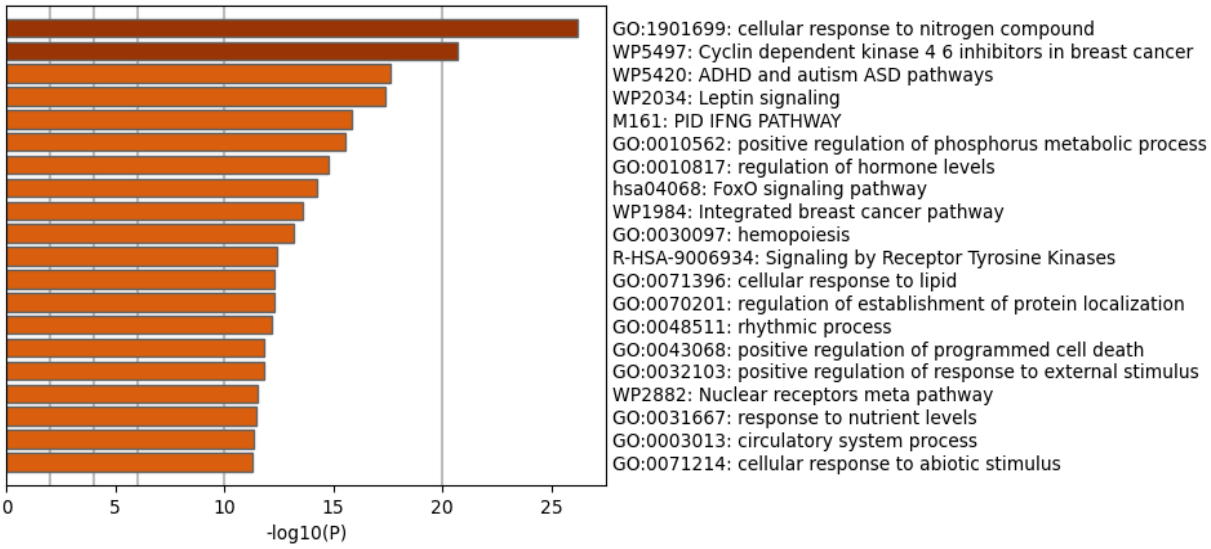

Figure 6D. Functional enrichment of MCODE-identified clusters derived from the lupeol–CMD PPI network, ranked by $-\log_{10}$(p-value)

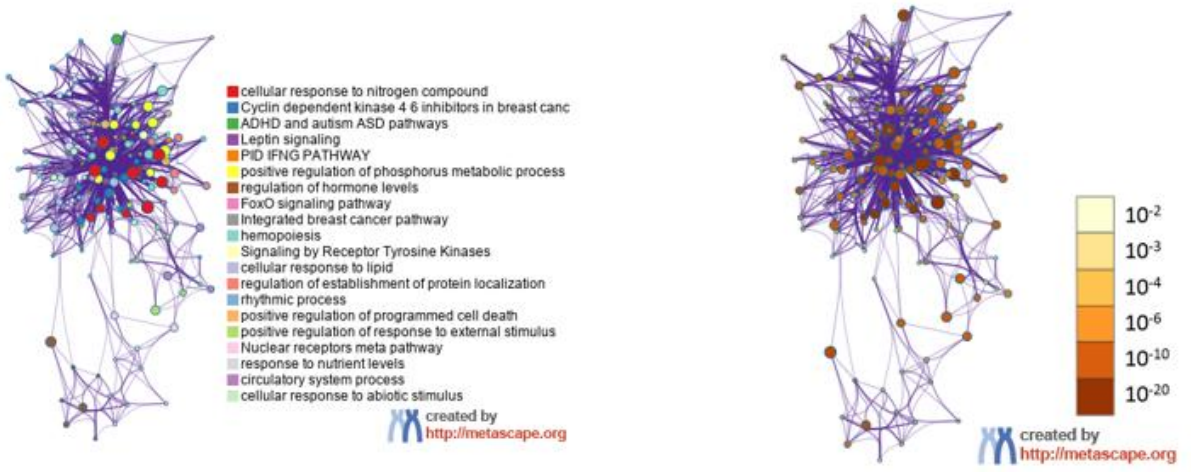

Figure 6E. Functional subnetwork visualization of enriched BP associated with lupeol–CMD targets. Colour gradients represent statistical significance levels

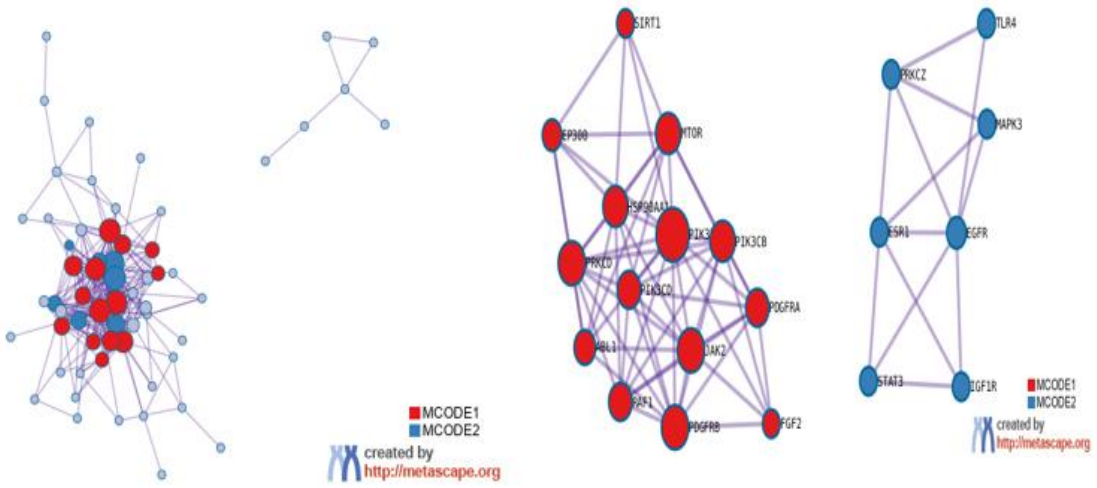

Figure 6F. PPI network illustrating MCODE-identified functional modules within the lupeol–CMD target set. Key hub proteins are centrally positioned within each module

Molecular docking analysis

To evaluate the binding affinity and interaction profiles of lupeol with key CMD–associated targets, molecular docking simulations were performed using Schrödinger Glide in standard precision (SP) mode. Docking scores (expressed in kcal/mol) were used as indicators of binding strength and interaction stability (Table 2). Lupeol exhibited favourable binding affinities toward multiple CMD-related protein targets, supporting its potential as a multi-target ligand. Among the analyzed targets, MAPK3 (−9.08 kcal/mol) and ESR1 (−9.03 kcal/mol) demonstrated the strongest binding energies, followed by CXCR4, FGF2, and EGFR, all of which exhibited docking scores below −8.0 kcal/mol. These results suggest a strong structural compatibility between lupeol and several proteins involved in metabolic, inflammatory, and vascular regulation.

Interaction pattern analysis of lupeol–target complexes

To further characterize the molecular basis of lupeol binding, the top ten docked protein–ligand complexes were analyzed for key interaction patterns, including hydrogen bonding, hydrophobic contacts, and π–alkyl interactions.

- MAPK3–lupeol complex showed dominant hydrophobic interactions within the ATP-binding pocket, contributing to its high binding affinity.
- ESR1–lupeol interaction was stabilized by hydrogen bonding and hydrophobic contacts within the ligand-binding domain, suggesting favourable receptor accommodation.
- CXCR4 and FGF2 complexes exhibited a combination of hydrophobic interactions and polar contacts, indicating stable ligand positioning within their respective binding cavities.
- EGFR–lupeol binding involved interactions with residues critical for kinase activity, supporting potential modulation of receptor signaling.

These interaction profiles collectively indicate that lupeol can engage multiple CMD-relevant targets through complementary binding modes rather than a single conserved interaction pattern.

Table 2. Docking scores of lupeol with selected CMD–related protein targets

Sr. No.	Target protein	Docking score (kcal/mol)
1	MAPK3	–9.08
2	ESR1	–9.03
3	CXCR4	–8.25
4	FGF2	–8.09
5	EGFR	–8.02
6	IGF1R	–7.94
7	JAK2	–7.90
8	KDR	–7.31
9	STAT3	–7.27
10	FGFR1	–6.08

Visualization of docked complexes

To visually examine lupeol–target interactions, multi-panel docking visualizations were generated for each selected protein, including two-dimensional interaction maps, surface views, and ribbon representations. Each target protein is represented by three panels (A–C), illustrating ligand orientation and interaction geometry. These visual analyses support the quantitative docking scores and provide structural insight into lupeol's multi-target binding behaviour. Table 3 depicts the docking poses of lupeol with MAPK3, ESR1, CXCR4, FGF2, EGFR, IGF1R, JAK2, KDR, STAT3, and FGFR1, respectively.

MD *Simulation of Lupeol–Target Complexes*

To investigate the dynamic stability and conformational behaviour of lupeol in complex with key CMD–associated targets, MD simulations were performed for 100 ns on five top-ranked protein–ligand complexes: CXCR4, EGFR, FGF2, ESR1, and MAPK3. Multiple trajectory descriptors were analyzed, including RMSD, RMSF, Rg, SASA, polar surface area (PSA), molecular surface area (MolSA), protein–ligand interaction profiles, and secondary structure elements (SSEs), to comprehensively assess complex stability under near-physiological conditions.

RMSD analysis

RMSD analysis was used to evaluate the overall structural stability of the protein–lupeol complexes throughout the 100 ns simulation period. The CXCR4–lupeol and FGF2–lupeol complexes stabilized early, with backbone RMSD values ranging between 1.5–2.2 Å and 1.8–2.6 Å, respectively. Ligand RMSD values remained below 2.5 Å, indicating sustained retention of lupeol within the binding pocket. The EGFR–lupeol complex exhibited moderate backbone flexibility (approximately 2.4–3.2 Å), while the ligand RMSD remained consistently aligned between 2.5–3.0 Å (Figure 7). In contrast, ESR1 showed higher backbone fluctuations (approximately 3.0–4.3 Å), consistent with the intrinsic flexibility of nuclear receptors; however, lupeol achieved stable positioning during the latter half of the simulation. The MAPK3–lupeol complex initially exhibited ligand displacement, with ligand RMSD values increasing up to approximately 12.0 Å during the early simulation phase.

Table 3. Multi-panel docking interaction visualizations of lupeol with CMD-related protein targets. Panel A: 2D interaction diagram highlighting hydrogen bonds and hydrophobic contacts. Panel B: Surface representation illustrating ligand accommodation within the binding pocket. Panel C: Ribbon representation showing overall protein–ligand orientation

Protein name	2D View (A)	Surface view (B)	Ribbon view (C)
MAPK3	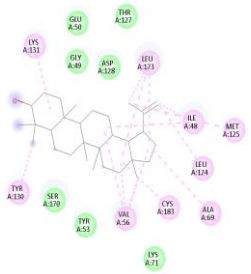	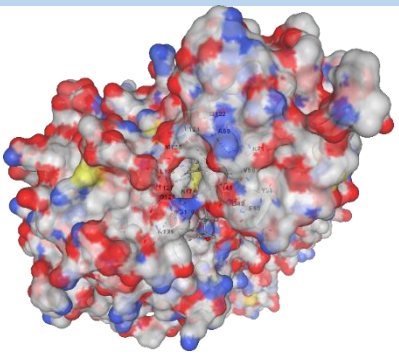	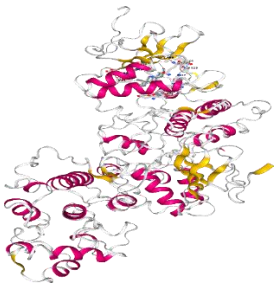
ESR1	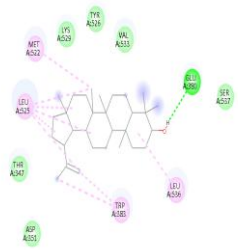	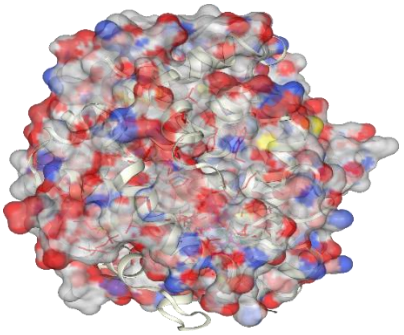	
CXCR4	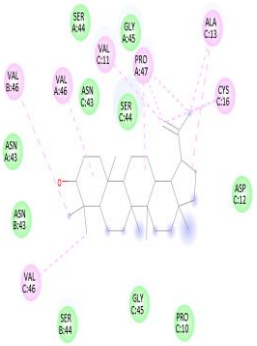	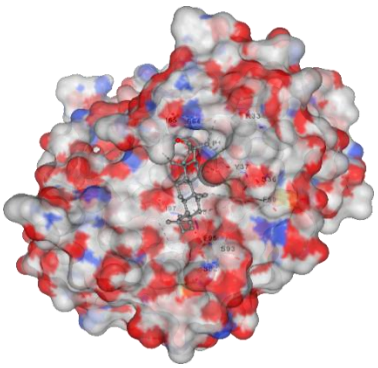	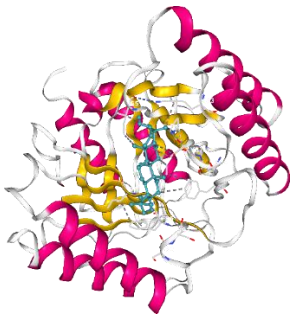
FGF2	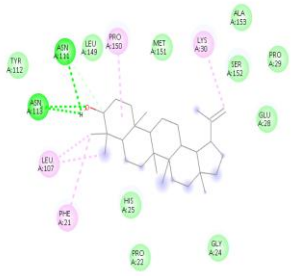	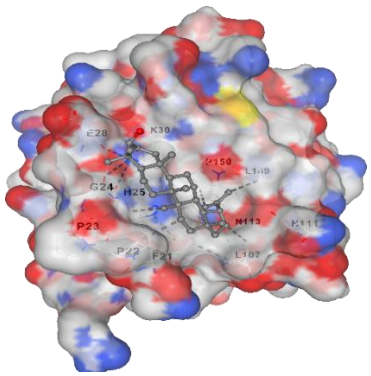	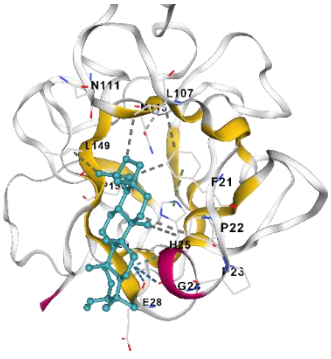

Protein name	2D View (A)	Surface view (B)	Ribbon view (C)
EGFR	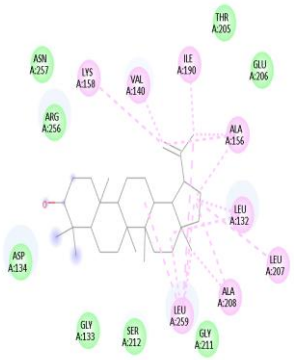	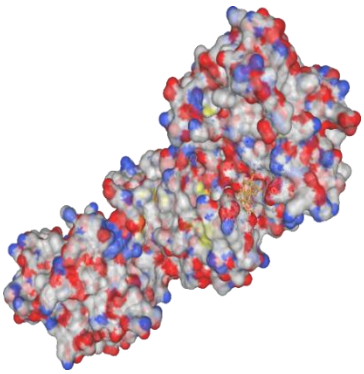	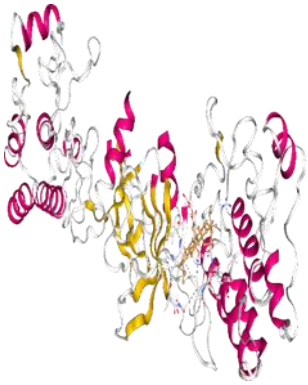
IGF1R	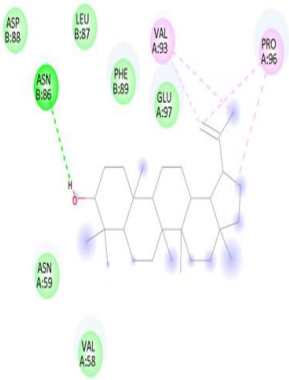	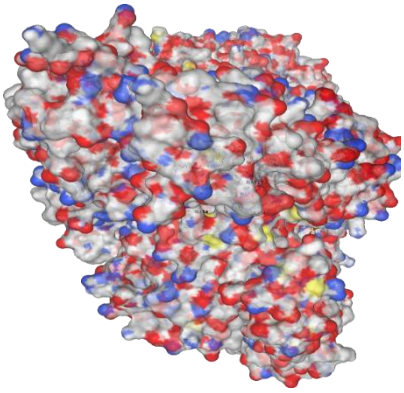	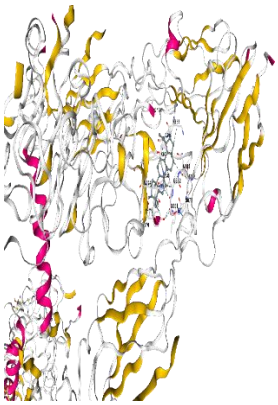
JAK2	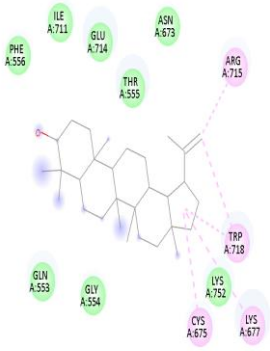	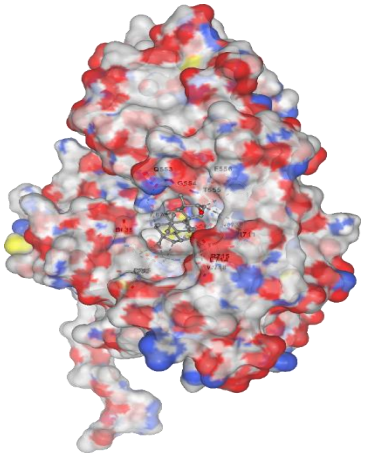	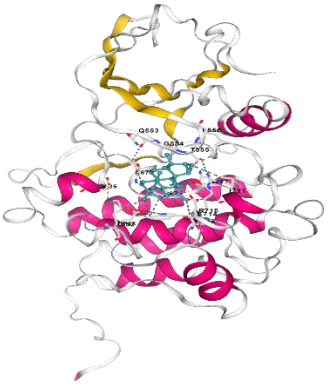

Protein name	2D View (A)	Surface view (B)	Ribbon view (C)
KDR	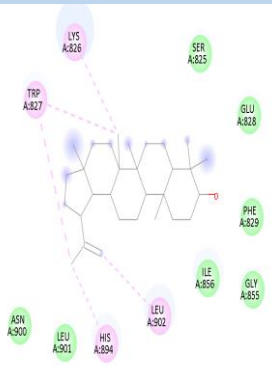	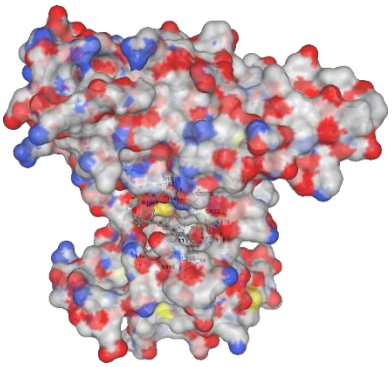	
STAT3	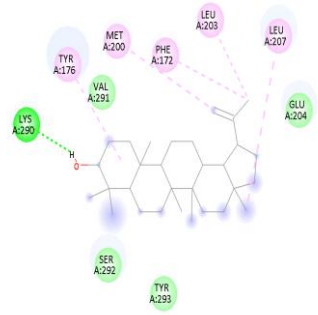	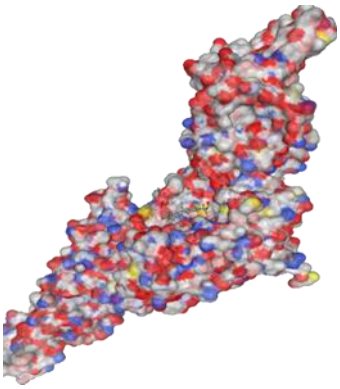	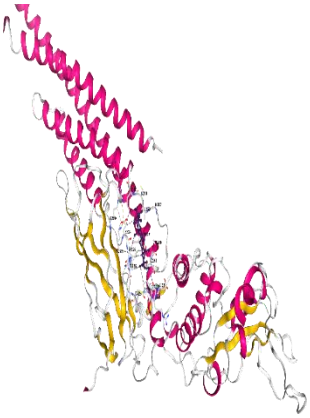
FGFR1	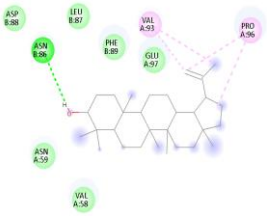	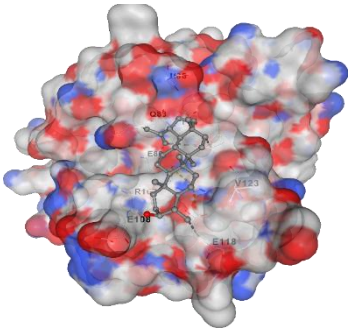	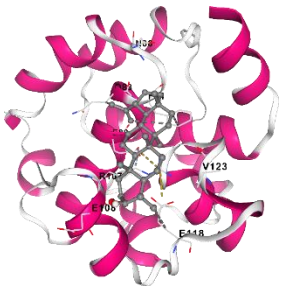

Subsequent stabilization was observed after approximately 40 ns, with ligand RMSD values converging around 6.0 Å, suggesting reorientation and stable rebinding within the binding region.

RMSF analysis

RMSF analysis was performed to assess residue-level flexibility within the protein–lupeol complexes, as shown in Figure 8.

For CXCR4, MAPK3, and EGFR, higher RMSF values (4.5–5.3 Å) were observed predominantly in terminal and loop regions, reflecting intrinsic protein flexibility.

Importantly, residues involved in ligand binding exhibited minimal fluctuations (<1.5 Å) across all complexes, indicating stable ligand–protein interactions. ESR1 and FGF2 also displayed localized flexibility outside the ligand-binding regions, while maintaining structural integrity at the interaction interface.

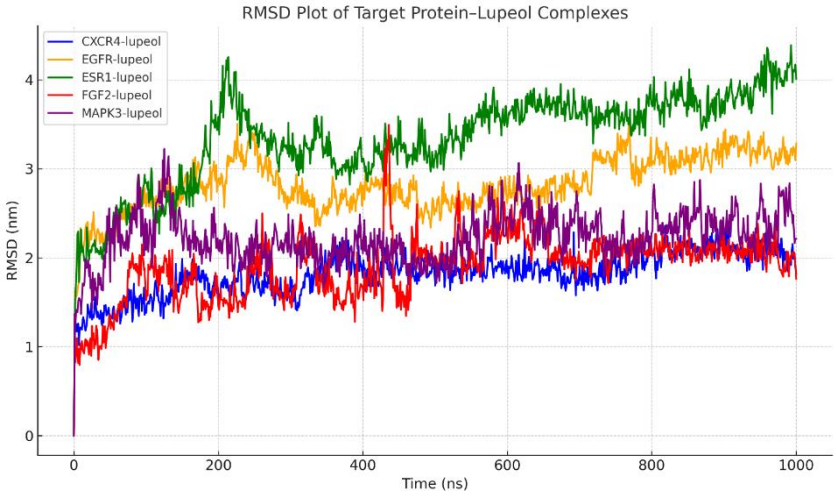

Figure 7. RMSD profiles of protein backbone (Cα atoms) and lupeol ligands for CXCR4, EGFR, ESR1, FGF2, and MAPK3 over 100 ns MD simulations. All complexes reached equilibrium within the early or mid-simulation phase and maintained acceptable stability throughout the trajectory

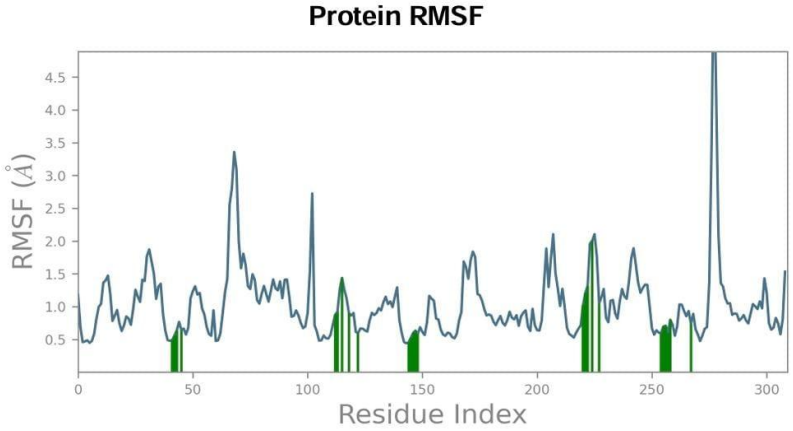

(a)

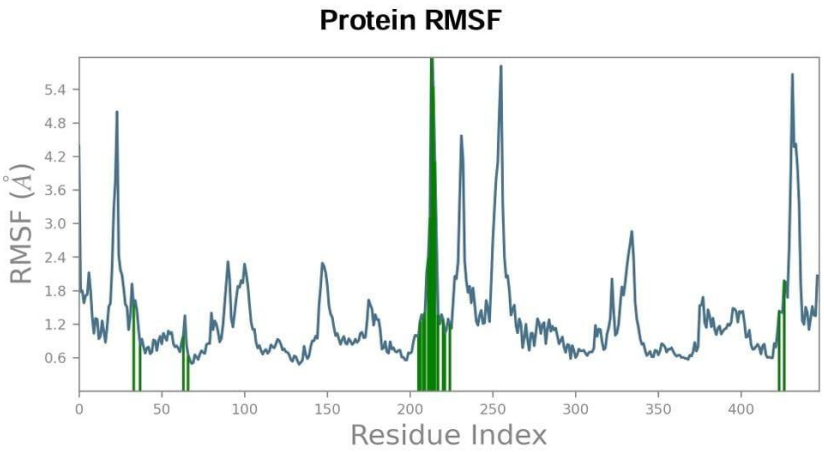

(b)

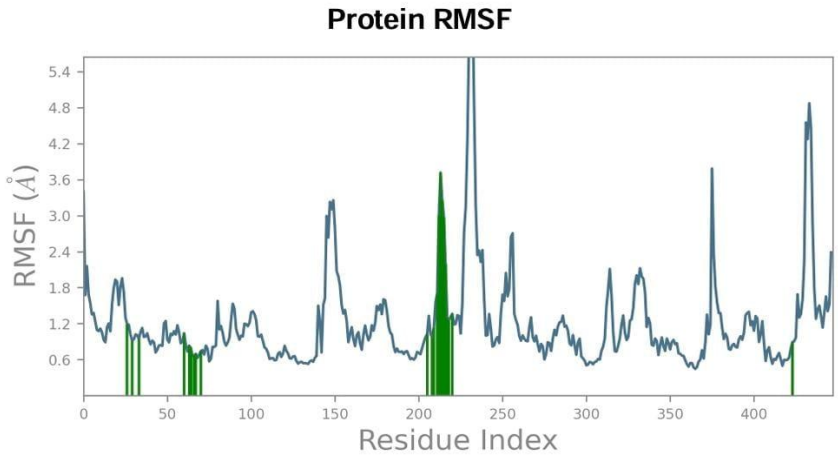

(c)

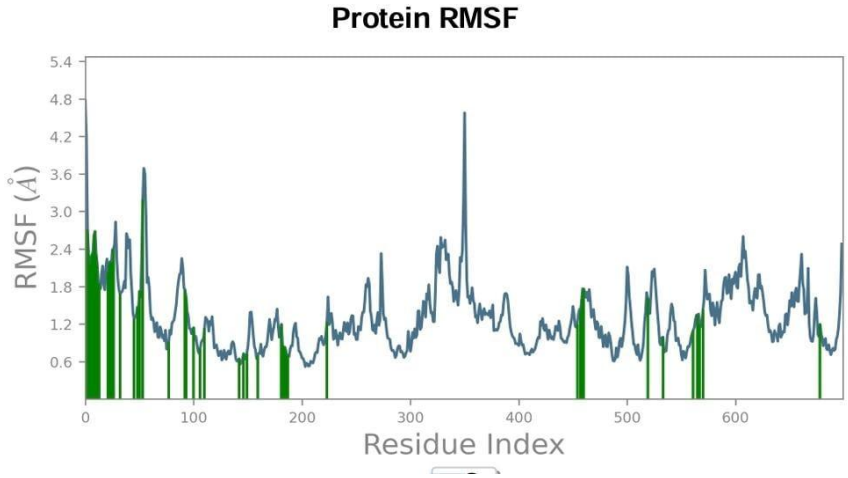

(d)

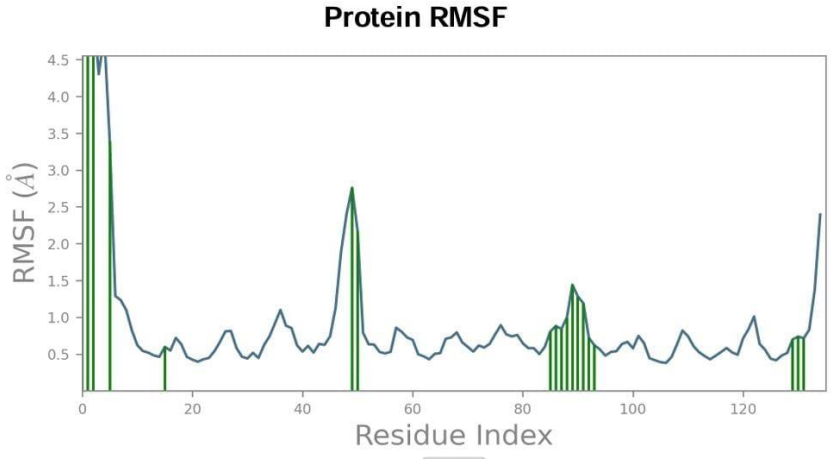

(e)

Figure 8. RMSF profiles of protein residues for lupeol complexes with (a) CXCR4, (b) EGFR, (c) ESR1, (d) FGF2, and (e) MAPK3. Residues involved in persistent ligand contact are indicated, demonstrating reduced flexibility within binding regions

Rg, SASA, PSA, and MolSA analysis

The Rg was analyzed to evaluate the compactness of the protein–ligand complexes. Across all systems, Rg values remained within a narrow range (3.2–3.5 Å), indicating the absence of large-scale structural unfolding. The EGFR– and ESR1–lupeol complexes exhibited slightly lower Rg values, suggesting relatively compact conformations. SASA analysis revealed lower solvent exposure for EGFR and ESR1 complexes (approximately 115–125 $Å^2$), consistent with deeper ligand burial within the binding pocket. In contrast, MAPK3 displayed relatively higher SASA values (~approximately 160 $Å^2$), reflecting partial surface-level interaction or dynamic binding behavior.PSA values ranged between 65 and 78 $Å^2$, with higher values observed for CXCR4 and EGFR, likely due to polar interactions at the binding interface. MolSA values remained stable (approximately 280–300 $Å^2$) across all complexes, indicating structural conservation of lupeol during the simulation. Time-dependent profiles of RMSD, Rg, MolSA, SASA, and PSA for lupeol complexes are illustrated in Figure 9.

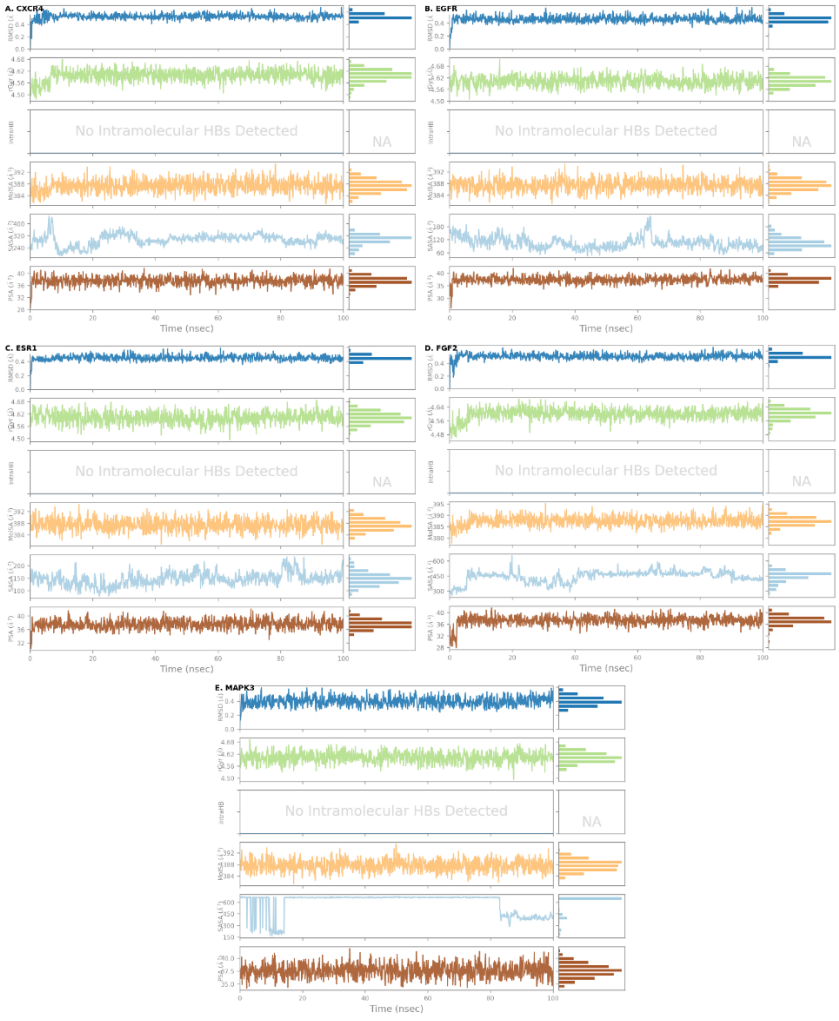

Figure 9. Time-dependent profiles of RMSD, Rg, MolSA, SASA, and PSA for lupeol complexes with CXCR4, EGFR, ESR1, FGF2, and MAPK3 over 100 ns MD simulations. Stable trends across parameters indicate sustained complex integrity of lupeol within the binding pocket. Variations in SASA reflect solvent exposure differences across protein systems

Protein–ligand interaction analysis

Protein–ligand interaction fraction analysis was conducted to identify residues contributing to stable binding over the simulation period (Figure 10). In the EGFR–lupeol complex, residues GLU_380 and TYR_526 formed persistent polar and hydrophobic interactions, respectively. The ESR1–lupeol complex displayed hydrogen bonding interactions with ASN_532 and VAL_534, supporting stable receptor engagement. In CXCR4, ASN_43 and GLY_45 contributed to hydrogen bonds and water-mediated interactions, while FGF2 interactions were dominated by hydrophobic contacts with transient water bridges. The MAPK3–lupeol complex showed more distributed hydrophobic interactions, which became more persistent during the latter half of the simulation, correlating with ligand stabilization observed in RMSD analysis.

SSE stability

SSE analysis was performed to assess whether lupeol binding influenced protein folding stability (Figure 11). EGFR and ESR1 maintained more than 60% SSE content, preserving their α-helical architecture throughout the simulation. CXCR4 retained its characteristic GPCR fold (53.68% SSE), while FGF2 preserved its β-trefoil structure. MAPK3 exhibited minor fluctuations in loop regions, but the kinase core remained structurally intact. No significant loss of secondary structural elements was observed, indicating that lupeol binding did not induce destabilizing conformational changes in the target proteins.

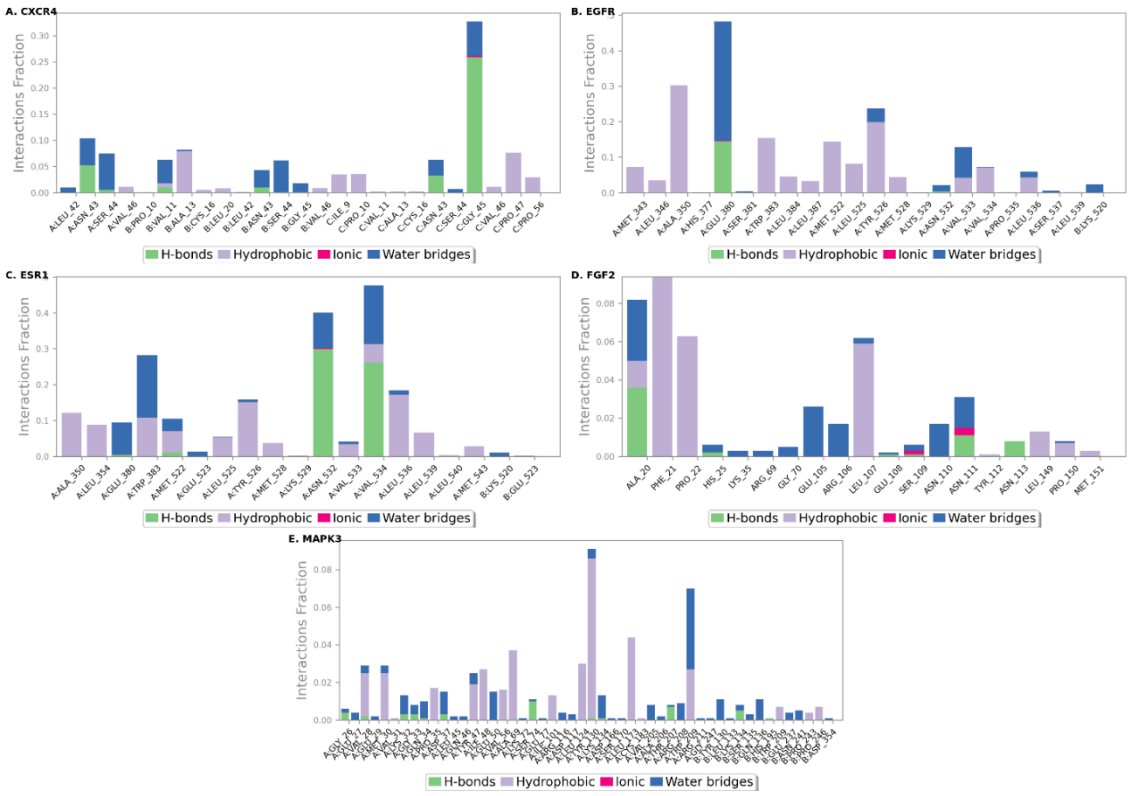

Figure 10. Protein–ligand interaction profiles illustrating interaction frequency and type (hydrogen bonds, hydrophobic contacts, ionic interactions, and water bridges) between lupeol and CMD-relevant targets over 100 ns simulations

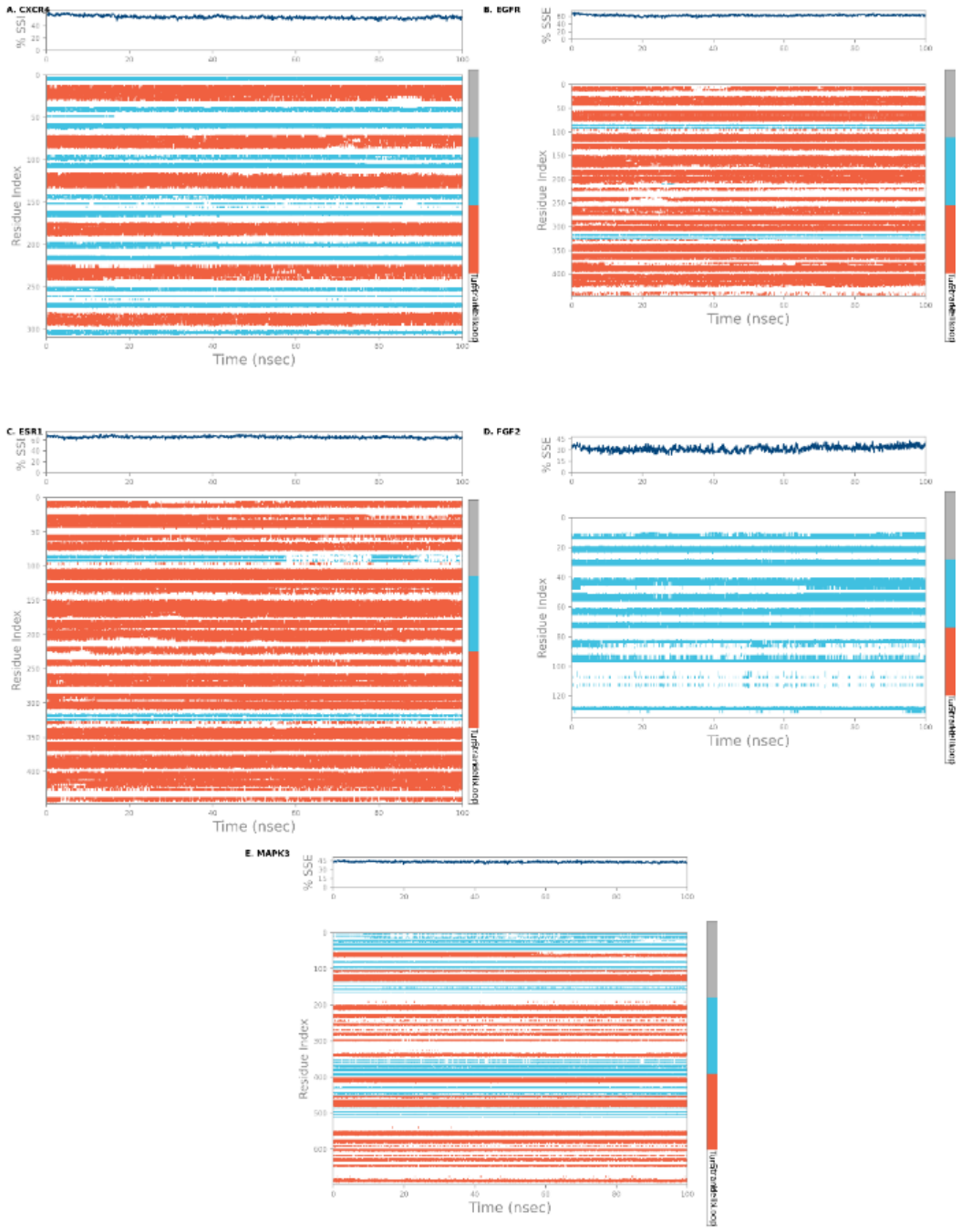

Figure 11. SSE stability plots showing the percentage and distribution of α-helices and β-strands for lupeol-bound protein complexes over 100 ns MD simulations. Consistent SSE profiles indicate preserved protein structural integrity

Tissue-specific expression of core target genes

To further validate the biological relevance of lupeol's predicted targets in the context of CMDs, their tissue-specific expression was analyzed using the Human Protein Atlas. Five hub genes—CXCR4, EGFR, FGF2, ESR1, and MAPK3—were examined across four CMD-relevant tissues: heart, liver, adipose tissue, and pancreas (Figure 12).

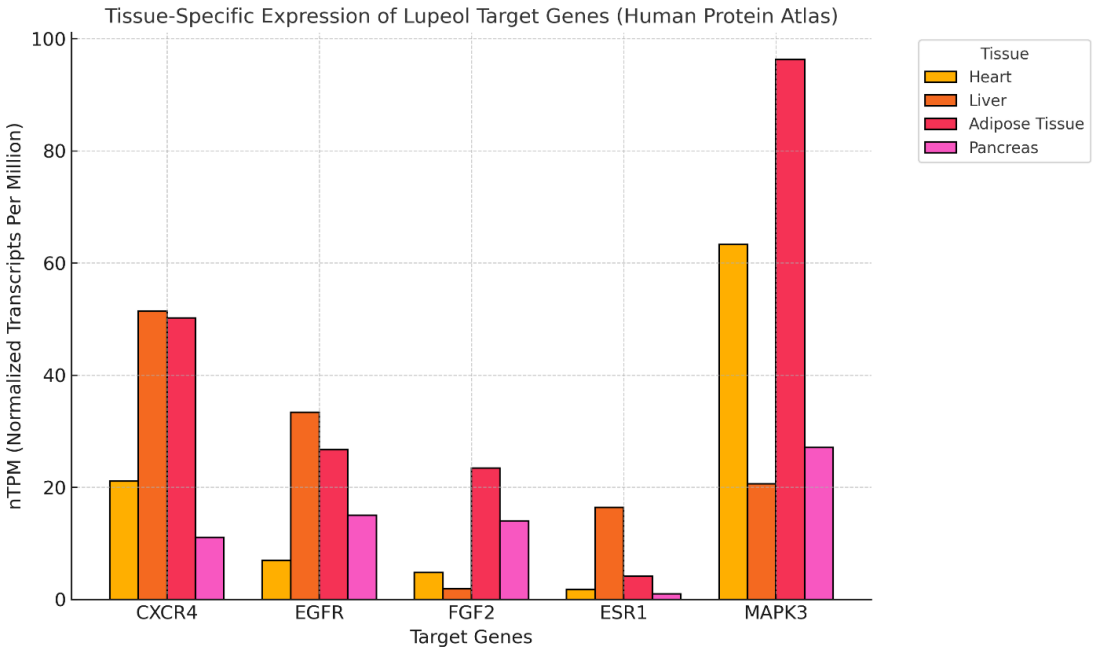

Figure 12. Tissue-specific expression profiles of selected lupeol target genes (CXCR4, EGFR, FGF2, MAPK3, and ESR1) across key metabolic and cardiovascular-related tissues. Expression levels (nTPM) were obtained from the Human Protein Atlas. Notably, MAPK3 showed high expression in adipose tissue (96.3 nTPM) and heart (63.3 nTPM), while CXCR4 and EGFR were elevated in liver and adipose tissue. ESR1 was moderately expressed in the liver and minimally in the heart and pancreas, suggesting variable regulatory roles

Discussion

CMDs represent a complex cluster of interrelated metabolic and cardiovascular disorders, including T2DM, obesity, dyslipidemia, hypertension, and CAD. These conditions share overlapping pathogenic mechanisms such as chronic low-grade inflammation, oxidative stress, insulin resistance, endothelial dysfunction, and metabolic dysregulation. Given this multifactorial nature, therapeutic strategies targeting single molecular entities often provide incomplete disease control, highlighting the need for multi-target approaches capable of modulating interconnected biological networks. In the present study, an integrated computational framework combining network pharmacology, molecular docking, ADME–toxicity prediction, and MD simulations was employed to explore the potential multi-target regulatory role of lupeol in CMDs. Rather than focusing on isolated targets, this systems-level strategy was designed to capture the complex interaction landscape underlying cardiometabolic pathology.

Lupeol demonstrates strong target overlap with CMD pathology

Network pharmacology analysis identified 179 overlapping targets between lupeol-associated proteins and CMD-related genes, suggesting broad target engagement across cardiometabolic pathways. PPI network analysis further highlighted STAT3, ESR1, MAPK3, JAK2, GSK3B, and EGFR as high-degree hub genes, indicating their central positions within the interaction network. These proteins are widely recognized regulators of inflammatory signaling, insulin sensitivity, lipid metabolism, and vascular function, processes that are critically dysregulated in CMDs. Importantly, the identification of these hub targets does not imply direct therapeutic efficacy, but rather suggests

that lupeol may influence CMD progression through coordinated modulation of multiple regulatory nodes. This observation aligns with emerging evidence that phytochemicals often exert pleiotropic effects by interacting with signaling networks rather than single molecular targets.

Pathway enrichment supports mechanistic link to CMDs

GO and KEGG pathway enrichment analyses revealed that lupeol-associated CMD targets were significantly enriched in PI3K–Akt, MAPK, AGE–RAGE, JAK–STAT, FoxO, and insulin signaling pathways. These pathways play pivotal roles in regulating glucose homeostasis, inflammatory responses, oxidative stress, endothelial integrity, and cell survival. Among these, PI3K–Akt signaling emerged as a central pathway, consistent with its established role in insulin signaling and cardiometabolic regulation. Dysregulation of this pathway has been implicated in insulin resistance, diabetic cardiomyopathy, and vascular dysfunction. The enrichment of lupeol-associated targets within this pathway suggests potential mechanistic relevance, although experimental validation is required to confirm pathway-level modulation.

Lupeol exhibits favourable ADME-tox and drug-likeness profiles

In silico ADME–toxicity predictions indicated that lupeol possesses high predicted intestinal absorption, acceptable drug-likeness, and a favourable safety profile, including non-mutagenicity, non-hepatotoxicity, and lack of hERG channel inhibition. These properties are particularly important for chronic cardiometabolic conditions that require long-term therapeutic management. However, lupeol's low aqueous solubility, characteristic of lipophilic triterpenoids, may limit its bioavailability, suggesting that formulation strategies such as nano-delivery systems or lipid-based carriers may be necessary for translational applications. These pharmacokinetic considerations highlight both the promise and limitations of lupeol as a lead compound, rather than a ready-to-use therapeutic agent.

Molecular docking confirms strong affinity to key CMD targets

Molecular docking analysis demonstrated that lupeol exhibits favourable binding affinities toward multiple CMD-associated targets, including MAPK3, ESR1, CXCR4, EGFR, and FGF2. Docking scores below −8.0 kcal/mol suggest energetically favourable ligand–protein interactions, supported by hydrogen bonding and hydrophobic contacts within the binding pockets. It is important to emphasize that docking scores represent theoretical binding tendencies rather than direct biological activity. Nevertheless, the ability of lupeol to engage structurally diverse targets supports the hypothesis that it may act through multi-target interaction mechanisms, which are increasingly recognized as advantageous in complex diseases such as CMDs.

Functional modules reveal therapeutic mechanisms

MCODE clustering and subnetwork analysis identified key functional modules enriched in neuroactive ligand-receptor interaction, leptin signaling, and cytokine–cytokine receptor pathways, all of which are implicated in metabolic inflammation and vascular remodeling. Hub genes such as STAT3, FGFR1, EGFR, and ESR1 were part of these modules, reinforcing their significance as central regulators. These pathways contribute to insulin resistance, endothelial dysfunction, and chronic inflammation, key hallmarks of CMD progression.

MD *confirms complex stability*

MD simulations provided further insight into the temporal stability and conformational behaviour of lupeol–protein complexes under near-physiological conditions. RMSD, RMSF, Rg, and solvent accessibility analyses collectively indicated that most lupeol–target complexes achieved stable conformations during the simulation period, without inducing significant structural destabilization of the proteins. Notably, ligand stabilization following initial fluctuations observed in certain complexes (*e.g.,* MAPK3) suggests adaptive binding behaviour rather than persistent instability. The preservation of secondary structural elements across simulations further supports the structural compatibility of lupeol with these targets; although such findings should be interpreted as supportive rather than conclusive evidence of functional modulation.

Tissue-specific expression profiles of selected lupeol target genes.

Tissue-specific expression analysis revealed that key hub targets, including MAPK3, CXCR4, EGFR, and ESR1, are expressed in CMD-relevant tissues such as the heart, liver, adipose tissue, and pancreas. This spatial expression pattern provides additional biological context, suggesting that the predicted targets are not only computationally relevant, but also physiologically expressed in organs central to cardiometabolic regulation. Nevertheless, expression alone does not equate to functional relevance, and the extent to which lupeol influences these targets *in vivo* remains to be established through experimental studies.

Conclusion and Future Perspectives

The present study provides a comprehensive network-based exploration of lupeol's pharmacological efficacy against CMDs (CMDs) by integrating network pharmacology, computational docking, ADME-tox profiling, and MD simulations. The findings demonstrate that lupeol exerts multitarget activity by modulating key genes and regulatory pathways central to CMD pathogenesis, including MAPK3, ESR1, EGFR, and CXCR4. Its strong binding potential, stable ligand–target interactions, and favourable pharmacokinetic and safety profiles further underscore its viability as a promising lead compound. Importantly, tissue-specific expression analysis demonstrated the functional relevance of lupeol's targets in key organs such as the heart, liver, pancreas, and adipose tissue critical nodes in CMD progression. These results not only validate lupeol's mechanistic involvement in metabolic and vascular regulation, but also highlight its potential for systemic therapeutic application. Future research should validate these computational predictions through *in vitro* and *in vivo* experiments, focusing on lupeol's efficacy in models of insulin resistance, dyslipidemia, and cardiac dysfunction. Furthermore, given lupeol's poor water solubility, formulation development using nanocarriers or lipid-based systems could enhance its bioavailability and therapeutic efficacy. Finally, clinical translation will require detailed toxicological assessments and pharmacodynamic studies in CMD patient populations. With further validation, lupeol holds significant promise as a multi-targeted, naturally derived therapeutic agent in the management of complex cardiometabolic disorders.

Disclosure Statement

No potential conflict of interest was reported by the authors.

ORCID

Pavithra Velusamy:
https://orcid.org/0000-0002-5032-6899
S. Rani:
https://orcid.org/0000-0002-6812-0450

G. Ariharasivakumar:
https://orcid.org/0000-0002-1533-6530

References

[1] Mensah, G.A., Roth, G.A., Fuster, V. The global burden of cardiovascular diseases and risk factors: 2020 and beyond. *Journal of the American College of Cardiology*, **2019**, 74(20), 2529-2532.

[2] Zhang, H., Duan, X., Rong, P., Dang, Y., Yan, M., Zhao, Y., Chen, F., Zhou, J., Chen, Y., Wang, D. Effects of potential risk factors on the development of cardiometabolic multimorbidity and mortality among the elders in china. *Frontiers in Cardiovascular Medicine*, **2022**, 9, 966217.

[3] Gong, W., Sun, P., Li, X., Wang, X., Zhang, X., Cui, H., Yang, J. Investigating the molecular mechanisms of resveratrol in treating cardiometabolic multimorbidity: A network pharmacology and bioinformatics approach with molecular docking validation. *Nutrients*, **2024**, 16(15), 2488.

[4] Patel, A. Effects of a fixed combination of perindopril and indapamide on macrovascular and microvascular outcomes in patients with type 2 diabetes mellitus (the advance trial): A randomised controlled trial. *The Lancet*, **2007**, 370(9590), 829-840.

[5] Choudhury, H., Pandey, M., Hua, C.K., Mun, C.S., Jing, J.K., Kong, L., Ern, L.Y., Ashraf, N.A., Kit, S.W., Yee, T.S. An update on natural compounds in the remedy of diabetes mellitus: A systematic review. *Journal of Traditional and Complementary Medicine*, **2018**, 8(3), 361-376.

[6] Saleem, M. Lupeol, a novel anti-inflammatory and anti-cancer dietary triterpene. *Cancer Letters*, **2009**, 285(2), 109-115.

[7] Siddique, H.R., Saleem, M. Beneficial health effects of lupeol triterpene: A review of preclinical studies. *Life Sciences*, **2011**, 88(7-8), 285-293.

[8] Ul Haq, M.N., Shah, G.M., Gul, A., Foudah, A.I., Alqarni, M.H., Yusufoglu, H.S., Hussain, M., Alkreathy, H.M., Ullah, I., Khan, A.M. Biogenic synthesis of silver nanoparticles using phagnalon niveum and its in vivo anti-diabetic effect against alloxan-induced diabetic wistar rats. *Nanomaterials*, **2022**, 12(5), 830.

[9] Das, A.K., Hossain, U., Ghosh, S., Biswas, S., Mandal, M., Mandal, B., Brahmachari, G., Bagchi, A., Sil, P.C. Amelioration of oxidative stress mediated inflammation and apoptosis in pancreatic islets by lupeol in stz-induced hyperglycaemic mice. *Life Sciences*, **2022**, 305, 120769.

[10] Sun, J., Luo, S., Deng, J., Yang, H. Phytochemicals in chronic disease prevention. *Nutrients*, **2023**, 15(23), 4933.

[11] Esposito, F., Mandrone, M., Del Vecchio, C., Carli, I., Distinto, S., Corona, A., Lianza, M., Piano, D., Tacchini, M., Maccioni, E. Multi-target activity of hemidesmus indicus decoction against innovative hiv-1 drug targets and characterization of lupeol mode of action. *Pathogens and Disease*, **2017**, 75(6), ftx065.

[12] Hopkins, A.L. Network pharmacology: The next paradigm in drug discovery. *Nature Chemical Biology*, **2008**, 4(11), 682-690.

[13] Lionta, E., Spyrou, G., K Vassilatis, D., Cournia, Z. Structure-based virtual screening for drug discovery: Principles, applications and recent advances. *Current topics in Medicinal Chemistry*, **2014**, 14(16), 1923-1938.

[14] Adki, K.M., Laddha, A.P., Oza, M.J., Gaikwad, A.B., Kulkarni, Y.A. Terpenes and terpenoids in management of diabetes & cardiovascular diseases. *Phytotherapy in the Management of Diabetes and Hypertension: Volume 3*, **2020**, 127-165.

[15] Sabarathinam, S., Satheesh, S. Unveiling the molecular mechanisms and clinical implications of maslinic acid in diabetes mellitus: Insights from network pharmacology. *Aspects of Molecular Medicine*, **2025**, 5, 100060.

[16] Sharma, N., Palia, P., Chaudhary, A., Verma, K., Kumar, I. A review on pharmacological activities of lupeol and its triterpene derivatives. *Journal of Drug Delivery & Therapeutics*, **2020**, 10(5).

[17] Aliyah, A.N., Ardianto, C., Samirah, S., Nurhan, A.D., Marhaeny, H.D., Ming, L.C., Khotib, J. In silico molecular docking study from moringa oleifera and caesalpinia sappan l. Secondary metabolites as antagonist trpv1. *Journal of Medicinal and Pharmaceutical Chemistry Research*, **2023**, 5(10), 885-894.

[18] Tamboli, A., Tayade, S. In-depth investigation of berberine and tropane through computational screening as possible dpp-iv inhibitors for the treatment of T2DM. *Journal of Pharmaceutical*

Sciences and Computational Chemistry, **2025**, 1(1), 1-11.

[19] Sharma, N., Palia, P., Chaudhary, A., Verma, K., Kumar, I. A review on pharmacological activities of lupeol and its triterpene derivatives. *Journal of Drug Delivery & Therapeutics*, **2020**, 10(5).

[20] Oh, K.K., Adnan, M., Cho, D.H. Network pharmacology study on morus alba l. Leaves: Pivotal functions of bioactives on ras signaling pathway and its associated target proteins against gout. *International Journal of Molecular Sciences*, **2021**, 22(17), 9372.

[21] Setyarini, A.I., Winarsih, S., Barlianto, W., Kalsum, U., Nugrahenny, D., Wiyasa, I.W.A. Network pharmacology and molecular docking analysis of phytoestrogens in vigna unguiculata for menopause treatment via interactions with erα, erβ, egfr, col1a1, and nos3. *Journal of Medicinal and Pharmaceutical Chemistry Research*, **2025**, 7(10), 2145-2160.

[22] Alqaraleha, M., Kasabrib, V., Muhanac, F., Al-Najjarc, B.O., Khleifatd, K.M. Evaluation of the antiproliferative activity and molecular docking of selected branched fatty acids. *Journal of Medicinal and Pharmaceutical Chemistry Research*, **2024**, 6(9), 1340-1353.

[23] Alabady, A.A., Al Majidi, S.M. Synthesis, characterization and evaluation molecular docking, and experimented antioxidant activity of some newchloroazetidine-2-one and diazetine-2-one derivatives from 2-phenyl-3-amino-quinazoline-4 (3h)-one. *Journal of Medicinal and Pharmaceutical Chemistry Research*, **2023**, 5(1), 1-18.

[24] Jangwan, N.S., Khan, M., Das, R., Altwaijry, N., Sultan, A.M., Khan, R., Saleem, S., Singh, M.F. From petals to healing: Consolidated network pharmacology and molecular docking investigations of the mechanisms underpinning rhododendron arboreum flower's anti-nafld effects. *Frontiers in Pharmacology*, **2024**, 15, 1366279.

HOW TO CITE THIS ARTICLE

P. Velusamy, S. Rani, G. Ariharasivakumar. Computational Multi-Target Profiling of Lupeol against Cardiometabolic Diseases: An Integrated Docking, Network Pharmacology, and Molecular Dynamics Approach. *Adv. J. Chem. A*, 2026, 9(6), 1128-1154.

DOI: 10.48309/AJCA.2026.545279.1984
URL: https://www.ajchem-a.com/article_238868.html